Sequenced Ethylene−Propylene Copolymers: Effects of Short Ethylene Run Lengths

Travis W. Baughman, John C. Sworen, and Kenneth B. Wagener*

The George and Josephine Butler Polymer Research Laboratory, Department of Chemistry, University of Florida, Gainesville, Florida 32611-7200

Received February 7, 2006; Revised Manuscript Received May 18, 2006

ABSTRACT: Two sequenced ethylene−propylene (EP) copolymers possessing methyl groups every fifth (EP5) or seventh (EP7) carbon have been prepared using an olefin metathesis polycondensation/hydrogenation strategy, thus generating methyl branched polyolefins with short ethylene run lengths of 4 or 6 carbons, respectively. Precise spacing of methyl branches along both copolymer backbones imparts pristine microstructure and targeted comonomer ratios in the copolymer. Extensive NMR spectral data are presented detailing polymer microstructure, branching analysis, and end-group identification. Thermal analysis using differential scanning calorimetry revealed multiple low-temperature relaxations for EP7 and glass transition temperature of −63 °C for EP5, and FT-IR analysis suggests no crystallinity under ambient conditions. A new ADMET monomer synthesis is also reported for the development of highly functionalized polyolefins or sequenced ethylene copolymers.

Introduction

Sixty years of research on polyolefin structure and crystallization has created volumes of data regarding the effect of polymer branching on material properties.[1−4] Although pendant alkyl branches, such as methyl groups, have been shown to reside both within polymeric crystals and throughout the amorphous regions of bulk materials,[5−9] both radical initiated and chain growth polymerizations lead to creation of irregular methylene sequence lengths between these branches, thereby reducing the propensity for polyolefin crystallization. Because of variable lengths of uninterrupted, easily crystallizable ethylene sequences in the material, semicrystalline polyolefins exhibit a distribution of lamellar crystal thicknesses, producing complex morphologies and broad melting behaviors.[8−12] Examples of linear ethylene−propylene (EP) copolymers illustrate this point well, as methyl branching in these materials has produced a large variety of bulk manifestations—in the realm of brittle solids to adhesive liquids, with the final material response dependent on comonomer content, branch distribution, and polymerization mode. Despite the occurrence of chain-transfer side reactions that lead to imperfect microstructure,[13] the versatility of polyolefin production is clear as free radical,[14,15] Ziegler−Natta,[12,16−21] metallocene,[11,22−26] and/or late transition metal[26−29] polymerizations are used to target specific branching defects and elicit a wider range of potential applications.[1,4] For proper investigation of the structure−property relationship in polyolefins and to further clarify the role of alkyl branching in these materials, the synthesis of macromolecular architectures with precise control over both branch identity and distribution is necessary.

Recently, a family of sequenced EP copolymers with exact chemical repeat units were synthesized through a metathesis polymerization/hydrogenation approach.[30,31] First, acyclic diene metathesis (ADMET) produces an unsaturated copolymer with absolute control over alkyl branch identity and frequency along the polymer backbone;[32−34] subsequently, exhaustive hydrogenation of this material yields sequenced ethylene−α-olefin copolymer analogues unattainable through standard chain copolymerization techniques. Approaching ethylene−α-olefin copolymer synthesis in this fashion has yielded ethylene−propylene (EP),[7,8,35] ethylene−1-butene,[36] and ethylene−1-octene[37] materials exhibiting pristine microstructures with exact ethylene sequence length between branches. We now report the extension of our EP copolymer work and a new synthetic methodology that enables the creation of sequenced copolymers with shorter ethylene run lengths and higher branch content.

This report details the synthesis of two highly branched, yet sequenced, ethylene−propylene copolymers and the effects of short, monodisperse ethylene sequence length distributions on the spectroscopic and thermal behavior of EP materials. The EP copolymers described herein possess methyl branches that are evenly spaced along the PE backbone at every fifth or seventh carbon, yielding a controlled number of 4 or 6 methylene units, respectively, between each branch point. The creation of highly branched EP copolymers by ADMET chemistry required an alternate synthetic approach where diene monomers were produced, bearing two distinct methyl branch points. This methodology not only allows for creation of the sequenced EP copolymers presented here but also provides a technique for the preparation of highly branched polyethylenes or functionalized materials with a thermally stable hydrocarbon backbone.

Experimental Section

Materials. All materials were purchased from Aldrich and used as received unless otherwise specified. Schrock's molybdenum catalyst $[(CF_3)_2CH_3CO]_2$(N-2,6-C_6H_3-*i*Pr_2)Mo=CHC$(CH_3)_2$Ph was synthesized according to literature procedures.[38] Sodium hydride was purchased and used as a mixture with 60 wt % mineral oil to facilitate weighing and limit fire hazard. Unless otherwise stated, reactions were performed in flame-dried glassware under argon gas in tetrahydrofuran (THF) obtained from a nitrogen-pressurized Aldrich keg system with an inline activated alumina drying column.

Instrumentation and Analysis. All ^{1}H NMR (300 MHz) and ^{13}C NMR (75 MHz) spectra were recorded on a Varian Associates Mercury 300 spectrometer. Chemical shifts for ^{1}H and ^{13}C NMR were referenced to residual signals from $CDCl_3$ (^{1}H = 7.27 ppm and ^{13}C = 77.23 ppm) with 0.03% v/v TMS as an internal reference. Reported ^{13}C NMR data for EP copolymers were performed on

* Corresponding author. E-mail: wagener@chem.ufl.edu.

10.1021/ma0602876 CCC: $33.50
Published on Web 06/21/2006

25−30 mg/mL concentrations averaging no less than 5000 transients applying no Overhauser enhancements.

Thin-layer chromatography (TLC) was performed on EMD silica gel coated (250 μm thickness) glass plates. Developed TLC plates were stained with iodine absorbed on silica to produce a visible signature. Reaction progress and relative purity of crude products were monitored by TLC chromatography and ^{1}H NMR. Fourier transform infrared (FT-IR) measurements were conducted on polymer films cast from chloroform onto KBr plates using a Bruker Vector 22 infrared spectrophotometer. High-resolution mass spectral (HRMS) data were obtained on a Finnegan 4500 gas chromatograph/mass spectrometer using either the chemical ionization (CI) or electrospray ionization (ESI) mode.

Differential scanning calorimetry (DSC) was performed using a Perkin-Elmer DSC 7 equipped with a controlled cooling accessory (CCA-7) at a heating rate of 10 °C/min unless otherwise stated, and quench cooling was performed at 400 °C/min. Calibrations were made using indium and freshly distilled *n*-octane as the standards for peak temperature transitions and indium for the enthalpy standard. All samples were prepared in hermetically sealed pans (4−7 mg/sample) and were run using an empty pan as a reference. Thermogravimetric analysis (TGA) was performed on a Perkin-Elmer TGA-7 at 20 °C/min under a nitrogen atmosphere.

Gel permeation chromatography (GPC) was performed using a Waters Associates GPCV2000 liquid chromatography system with its internal differential refractive index detector (DRI) at 40 °C using two Waters Styragel HR-5E columns (10 μm PD, 7.8 mm i.d., 300 mm length) with HPLC grade THF as the mobile phase at a flow rate of 1.0 mL/min. Injections were made at 0.05−0.07% w/v sample concentration using a 220.5 μL injection volume. Retention times were calibrated against narrow molecular weight polystyrene standards (Polymer Laboratories, Amherst, MA) using a nine-point calibration.

Synthesis of EP7 Copolymer. Diethyl-2-(but-3-enyl) Malonate (1). 4-Bromo-1-butene (20.6 g, 153 mmol) was added to a stirred slurry of diethyl malonate (48.8 g, 305 mmol), sodium hydride (4.39 g, 183 mmol), and THF (120 mL) at 0 °C and allowed to stir for 30 min. The resultant mixture was heated to 60 °C for 8 h. After cooling to room temperature, the reaction was slowly quenched with water (150 mL) and finally concentrated HCl (∼10 mL) until acidic (pH ∼ 4). Column chromatography (1:3 diethyl ether: hexanes) afforded 25.2 g (77.2% yield) of colorless oil. ^{1}H NMR spectral data matched reported values.[39] ^{13}C NMR ($CDCl_3$): δ (ppm) 14.28, 28.05, 31.51, 51.42, 61.51, 116.14, 137.10, 169.63. CI/HRMS: $[M + H]^+$ calcd for $C_{21}H_{19}O_4$: 215.1283; found: 215.1282.

1,6-(Diethyl-2-(but-3-enyl)malonyl)hexane (2). Compound **1** (15.0 g, 70 mmol) was added to a slurry of sodium hydride (1.68 g, 70 mmol) in THF (75 mL) by syringe at 0 °C. 1,6-Dibromohexane (7.77 g, 32 mmol) was added slowly to the solution via syringe, and the mixture warmed to 65 °C for 8 h. Once cooled to room temperature, the reaction was subsequently quenched by slow addition of water (100 mL) and HCl (∼5 mL) until acidic (pH ∼ 4). Column chromatography (3:7 ethyl ether:hexanes) afforded 8.4 g (51.7% yield) of colorless oil. ^{1}H NMR ($CDCl_3$): δ (ppm) 1.09−1.33 (br, 20H), 1.87 (m, 4H), 1.95 (m, 8H), 4.17 (q, 8H), 5.02 (m, 4H), 5.78 (m, 2H). ^{13}C NMR ($CDCl_3$): δ (ppm) 14.29, 24.13, 28.57, 29.80, 31.69, 32.44, 57.42, 61.21, 115.10, 137.87, 171.86. CI/HRMS: $[M + H]^+$ calcd for $C_{28}H_{47}O_8$: 511.3276; found: 511.3271. Elemental analysis calcd for $C_{28}H_{46}O_8$: 65.86 C, 9.08 H; found: 65.66 C, 9.27 H.

2,9-(But-3-enyl)-2,9-dicarboxysebacic Acid (3). Potassium hydroxide (25.0 g, 446 mmol) was added to a mixture of **2** (20.0 g, 39 mmol) in ethanol (125 mL) and water (50 mL) at room temperature. The reaction mixture was heated at reflux for 2 h before cooling to room temperature. Diethyl ether (100 mL) followed by water (50 mL) and finally concentrated HCl (∼200 mL) were added over 30 min until acidic (pH ∼ 4). The biphasic mixture was transferred to a separatory funnel, extracted twice with diethyl ether (2 × 150 mL), washed with brine (2 × 150 mL), and concentrated to a hydrated yellow solid at 118% crude yield of a mixture of tetraacid and what seemed to be potassium chloride. No further purification was performed LSI/HRMS: $[M + Na]^+$ calcd for $C_{20}H_{30}O_8Na$: 421.1823; found: 421.1836. Elemental analysis calcd for $C_{20}H_{30}O_8$: 60.29 C, 7.59 H; found: 59.97 C, 7.67 H.

2,9-(But-3-enyl)sebacic Acid (4). Solid tetraacid **3** (24.8 g, 62 mmol) was mixed with Decalin (25 mL) and heated to 185 °C in a 250 mL round-bottom flask equipped with an air-cooled condenser connected to a mineral oil bubbler. The reaction was stirred vigorously until gas evolution ceased (typically 30 min at this scale). Upon cooling, decalin was removed via rotary evaporation, affording a yellow oil. Column chromatography (100% ethyl acetate) afforded 15.6 g (80.9% yield from **2**) of yellow oil. ^{1}H NMR ($CDCl_3$): δ (ppm) 1.20−1.89 (br, 16H), 2.10 (q, 4H), 2.39 (m, 2H), 5.02 (m, 4H), 5.79 (m, 2H), 11.74 (br, 1.5H). ^{13}C NMR ($CDCl_3$): δ (ppm) 27.33, 29.47, 31.45, 31.68, 32.23, 45.05, 115.43, 137.96, 183.01. LSI/HRMS: $[M + Na]^+$ calcd for $C_{18}H_{30}O_4Na$: 333.2057; found: 333.2048. Elemental analysis calcd for $C_{18}H_{30}O_4$: 69.64 C, 9.74 H; found: 68.69 C, 9.71 H.

2,9-(But-3-enyl)-1,10-decanediol (5). A solution of diacid **4** (8.7 g, 28 mmol) in THF was added dropwise to a slurry of LAH (10.6 g, 279 mmol) in diethyl ether at 0 °C. The mixture was warmed to 45 °C and stirred for 4 h. The reaction was quenched with successive additions of water (50 mL) and 6 N HCl (300 mL) over 30 min. The organic phase was collected in two ether (150 mL) washings, washed with brine (2 × 150 mL), and dried with $MgSO_4$. Filtration and solvent removal afforded an oil with a slight yellow hue. Column chromatography (3:7 hexanes:diethyl ether) yielded 6.2 g (78.2% yield) of colorless oil. ^{1}H NMR ($CDCl_3$): δ (ppm) 1.28−1.58 (br, 20H), 2.08 (q, 4H), 3.55 (d, 4H), 4.98 (m, 4H), 5.82 (m, 2H). ^{13}C NMR ($CDCl_3$): δ (ppm) 29.97, 30.14, 30.37, 31.01, 31.32, 40.14, 65.60, 114.58, 139.22. CI/HRMS: $[M + H]^+$ calcd for $C_{18}H_{35}O_2$: 283.2637; found: 283.2633. Elemental analysis calcd for $C_{18}H_{34}O_2$: 76.54 C, 12.13 H; found: 75.91 C, 12.01 H.

5,12-Dimethyldodeca-1,15-diene (6). A solution of diol **5** (3.78 g, 13 mmol) in triethylamine (5.0 mL, 49 mmol) and chloroform (75 mL) was cooled to 0 °C, and mesyl chloride (3.5 g, 31 mmol) was added dropwise via syringe over 5 min. The reaction mixture was warmed to room temperature and stirred for 1 h. The crude mixture was transferred to a separatory funnel and washed water (2 × 50 mL), 1 N HCl (2 × 50 mL), and saturated potassium carbonate (2 × 50 mL). Each washing was extracted with dichloromethane (50 mL). The chloroform and dichloromethane portions were combined, dried with $MgSO_4$, and concentrated to an orange oil.

A solution of crude dimesylate in diethyl ether (75 mL) was added dropwise, over a 20 min period, to a slurry of precooled (0 °C) of LAH (6.0 g, 158 mmol) in diethyl ether (150 mL). The reaction was warmed to room temperature and stirred for 1 h. Successive additions of water (6 mL), 15% NaOH (6 mL), and water (18 mL) followed by filtration and solvent removal yielded a biphasic, colorless mixture. Column chromatography (hexanes) isolated 2.3 g (68.7% yield) of colorless oil. ^{1}H NMR ($CDCl_3$): δ (ppm) 0.87 (d, 6H), 1.0−1.5 (br, 18H), 2.06 (m, 4H), 4.98 (m, 4H), 5.83 (m, 2H). ^{13}C NMR ($CDCl_3$): δ (ppm) 19.76, 27.24, 30.25, 31.62, 32.51, 36.48, 37.18, 114.13, 139.69. CI/HRMS: $[M]^+$ calcd for $C_{18}H_{34}$: 250.2661; found: 250.2669. Elemental analysis calcd for $C_{18}H_{34}$: 86.32 C, 13.68 H; found: 84.49 C, 13.52 H.

Polymerization of 5,12-Dimethylhexadeca-1,15-diene: EP7u (7). Prior to reaction, pure diene monomer **6** was successively vacuum-transferred onto a potassium metal mirror, allowed to stand for 4 h at room temperature, vacuum-transferred to a 50 mL Schlenk flask, and taken into an argon-filled glovebox. Diene monomer **6** (1.0 g) was added to Schrock's molybdenum catalyst (1500:1) and stirred until ethylene evolution slowed and the viscosity increased. The reaction flask was sealed with a Schlenk adapter, taken out of the glovebox, and fitted to a high-vacuum line. Vacuum was applied intermittently over 3 h during which noticeable viscosity increase of the golden amorphous liquid was observed. High vacuum (∼10^{-4} Torr) was applied, and the temperature increased to 40 °C for 72 h. The polymerization was quenched by opening the flask to the

atmosphere and adding toluene (25 mL). Upon dissolution, polymer solutions were stirred until a green color arose and finally flashed through a 2 in. plug of neutral silica to remove catalyst residue. Removal of solvent afforded a colorless liquid polymer. ^{1}H NMR ($CDCl_3$): δ (ppm) 0.85 (d, 6H), 1.02−1.45 (br, 18H), 1.99 (m, 4H), 5.33−5.45 (m, 2H). ^{13}C NMR ($CDCl_3$): δ (ppm) 19.81, 25.02, 27.28, 30.31, 30.41, 32.50, 32.65, 37.23, 37.34, 130.13 (cis olefin), 130.59 (trans olefin). FT-IR (cm^{-1}): 2963, 2925, 2850, 1462, 1376, 967, 722. Elemental analysis calcd for $C_{17}H_{32}$: 86.36 C, 13.64 H; found: 86.45 C, 13.79 H. Thermal decomposition under nitrogen at 10 °C/min: 10% weight loss at 417 °C.

EP7 (8). Unsaturated polymer **7** (~1.0 g) was dissolved in toluene (150 mL) and transferred to a Parr pressure reactor equipped with a glass sleeve and Teflon stirbar. Palladium (10 mol % on carbon) (100 mg) was added to the solution; the reactor was sealed, was purged three times with 1000 psi hydrogen gas, and filled to 1000 psi prior to heating the stirred contents to 120 °C for 72 h. The crude reaction mixture was vacuum-filtered over a 2 in. plug of silica to remove carbon residue. Subsequent removal of solvent gave 947 mg (95% mass yield from 1 g of **6**) of colorless, viscous liquid. ^{1}H NMR ($CDCl_3$): δ (ppm) 0.85 (d, 3H), 1.02−1.45 (br, 13.67H). ^{13}C NMR ($CDCl_3$): δ (ppm) 19.98, 27.37, 30.35, 33.01, 37.38. FT-IR (cm^{-1}): 2924, 2853, 1464, 1377, 723. Elemental analysis calcd for $C_{17}H_{34}$: 85.63 C, 14.37 H; found: 85.53 C, 14.66 H. Thermal decomposition under nitrogen at 10 °C/min: 10% weight loss at 315 °C.

Synthesis of EP5 Copolymer. Synthetic methodology to produce **EP5** is identical to that given previously for the total synthesis of the **EP7** copolymer.

1,4-(Diethyl-2-allylmalonyl)butane (9). Column chromatography (1:4 ethyl ether:hexanes) produced 9.6 g (58.7% yield) of a colorless oil. ^{1}H NMR ($CDCl_3$): δ (ppm) 1.12−1.26 (br, 16H), 1.79 (m, 4H), 2.58 (d, 4H), 4.14 (q, 8H), 5.05 (m, 4H), 5.59 (m, 2H). ^{13}C NMR ($CDCl_3$): δ (ppm) 14.22, 24.25, 32.07, 37.08, 57.42, 61.24, 118.93, 132.65, 171.33. CI/HRMS: $[M + H]^+$ calcd for $C_{24}H_{39}O_8$: 454.2678, found: 454.2671. Elemental analysis calcd for $C_{24}H_{38}O_8$: 63.42 C, 8.43 H; found: 63.30 C, 8.45 H.

2,7-Diallyl-2,7-dicarboxysuberic Acid (10). Product isolated as a hydrated mixture of tetraacid and what appeared to be potassium chloride in 113% crude yield. No further purification was performed. LSI/HRMS: $[M + Na]^+$ calcd for $C_{28}H_{47}O_8Na$: 365.1212; found: 365.1216. Elemental analysis calcd for $C_{16}H_{22}O_8$: 56.13 C, 6.48 H; found: 55.97 C, 6.38 H.

2,7-Diallylsuberic Acid (11). Column chromatography (ethyl acetate) isolated 13.2 g (74.7% yield from **9**) of yellow oil. ^{1}H NMR ($CDCl_3$): δ (ppm) 1.25−1.43 (br, 4H), 1.45−1.72 (br, 4H), 2.18−2.31 (m, 2H), 2.32−2.50 (m, 4H), 5.10 (m, 4H), 5.76 (m, 2H). ^{13}C NMR ($CDCl_3$): δ (ppm) 27.26, 31.37, 36.24, 36.31, 45.33, 117.27, 135.28, 182.55. LSI/HRMS: $[M + Na]^+$ calcd for $C_{14}H_{22}O_4Na$: 277.1416; found: 277.1410. Elemental analysis calcd for $C_{14}H_{22}O_4$: 66.12 C, 8.72 H; found: 66.11 C, 8.80 H.

2,7-Diallyl-1,8-octanediol (12). Column chromatography (15:85 hexanes:diethyl ether) yielded 4.5 g (71.2%) of a colorless oil. ^{1}H NMR ($CDCl_3$): δ (ppm) 1.32 (br, 8H), 1.61 (br, 4H), 2.11 (t, 4H), 3.54 (d, 4H), 5.05 (m, 4H), 5.81 (m, 2H). ^{13}C NMR ($CDCl_3$): δ (ppm) 27.41, 30.76, 36.00, 36.02, 40.59, 65.73, 116.39, 137.30. LSI/HRMS: $[M + H]^+$ calcd for $C_{14}H_{27}O_2$: 227.2011; found: 227.2009. Elemental analysis calcd for $C_{14}H_{26}O_2$: 74.29 C, 11.58 H; found: 74.14 C, 11.57 H.

4,9-Dimethyldodeca-1,11-diene (13). Column chromatography (hexanes) yielded 3.3 g (87.4% yield) of a colorless oil. ^{1}H NMR ($CDCl_3$): δ (ppm) 0.88 (d, 6H), 1.04−1.55 (br, 10H), 1.91 (m, 2H), 2.05 (m, 2H), 4.99 (m, 4H), 5.79 (m, 2H). ^{13}C NMR ($CDCl_3$): δ (ppm) 19.68, 27.58, 33.03, 36.84, 41.67, 41.69, 115.58, 138.01. CI/HRMS: $[M]^+$ calcd for $C_{14}H_{26}$: 194.2035; found: 194.2025. Elemental analysis calcd for $C_{14}H_{26}$: 86.52 C, 13.48 H; found: 86.34 C, 13.70 H.

Polymerization of 4,9-Dimethyldodeca-1,11-diene: EP5u (14). ^{1}H NMR ($CDCl_3$): δ (ppm) 0.85 (d, 6H), 1.02−1.52 (br, 10H), 1.84 (m, 2H), 1.98 (m, 2H), 5.36 (m, 2H). ^{13}C NMR ($CDCl_3$): δ (ppm) 19.76, 27.66, 33.45, 34.92, 35.73, 36.89, 40.41, 40.43, 129.46 (cis olefin), 130.31 (trans olefin). FT-IR (cm^{-1}): 3004, 2953, 2925, 2855, 2724, 1464, 1438, 1376, 968, 725. Elemental analysis calcd for repeat unit $C_{13}H_{24}$: 86.59 C, 13.41 H; found: 86.76 C, 13.38 H. Thermal decomposition under nitrogen at 10 °C/min; 10% weight loss at 375 °C.

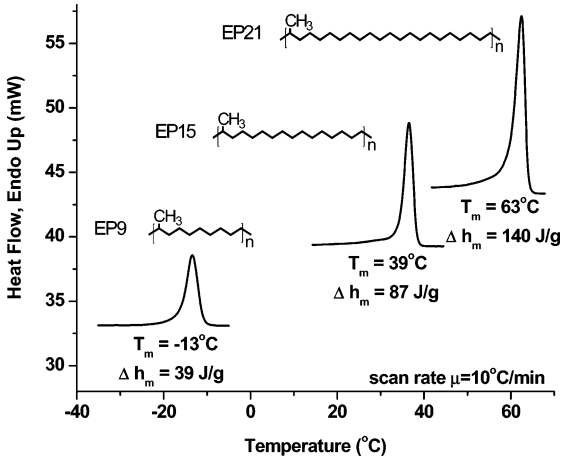

Figure 1. DSC thermograms of previously synthesized EP copolymers.

EP5 (15). Isolated as 984 mg (98% mass yield from 1.0 g of **13**) of colorless, viscous liquid. ^{1}H NMR ($CDCl_3$): δ (ppm) 0.85 (d, 3H), 1.02−1.43 (br, 9.19H). ^{13}C NMR ($CDCl_3$): δ (ppm) 19.99, 27.70, 33.03, 37.41. FT-IR (cm^{-1}): 2952, 2925, 2855, 2722, 1464, 1377, 1152, 727. Elemental analysis calcd for $C_{13}H_{26}$: 85.63 C, 14.37 H; found: 85.54 C, 14.60 H. Thermal decomposition under nitrogen at 10 °C/min; 10% weight loss at 275 °C.

Results and Discussion

Polymer Design and Synthesis. Sequenced EP copolymers have been produced using ADMET chemistry, affording a family of methyl branched polyethylenes (EP copolymers) with targeted comonomer ratios and precise branch placement.[35] To easily describe the sequenced copolymers in this document, the nomenclature is based on the parent chain-addition comonomers and branch frequency. For example, **EP21** begins with the prefix **EP** standing for ethylene (**E**) and propylene (**P**), the two comonomers, and the number **21** is the branch frequency along the polymer backbone. **EP21** can be considered a linear PE with a methyl branch on every 21st carbon or a sequenced EP copolymer with 9.5 units of ethylene between each propylene unit.

Synthesis of ADMET EP copolymers began with EP19 in 1997[40] followed by an extension of this theme to include EP9, -11, -15, and -21.[7,8,35] All of the aforementioned ADMET EP copolymers exhibit semicrystalline behavior, and for every copolymer, higher branch frequencies and shorter ethylene run lengths result in lower peak melting temperatures and heats of fusion.[8,35] Figure 1 illustrates a comparison of thermal responses for EP9, EP15, and EP21 highlighting their melting endotherms. Longer ethylene run lengths present in EP15 and EP21 lead to higher melting, more crystalline materials as lower methyl branch (defect) content along the polymer backbone promotes crystallization. As branch content increases in these EP copolymers, the ethylene run length decreases, thereby yielding less crystalline materials with lower peak melting temperatures; however, because of the precise placement of pendant methyl branches, even EP9, having the highest molar concentration of defects, still retains a relatively sharp melting profile. Before this report, our group had yet to synthesize an amorphous sequenced EP copolymer, even though comparable, randomly (or statistically) branched EP copolymers in the literature have shown both semicrystalline[12,41] and/or amorphous behavior.[28,29]

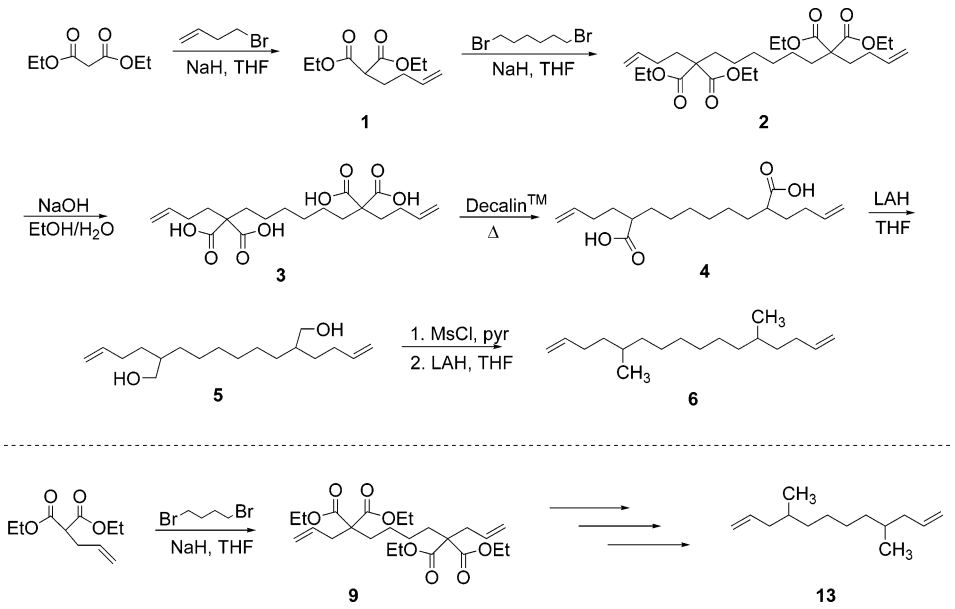

Figure 2. ADMET monomer synthesis.

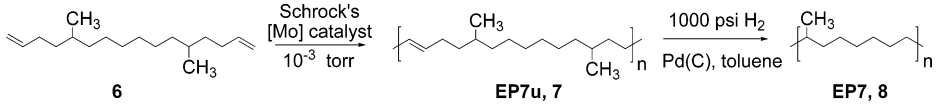

Figure 3. EP7 copolymer synthesis.

Table 1. Polymer Characterization Data

	mol % ethylene		mol % propylene		GPC data[c]				
polymer name	calcd[a]	NMR[b]	calcd[a]	NMR[b]	M_n	M_w	PDI[d]	onset of decomposition[e] (°C)	methyl branch density[f]
EP5u					26.0	45.7	1.8	375	
EP5	60.0	60.7	40.0	39.3	28.4	47.6	1.7	275	200 (197)
EP7u					12.7	20.3	1.6	417	
EP7	71.4	72.3	28.6	27.3	12.9	20.3	1.6	315	143 (137)

[a] Calculated from expected polymer repeat unit. [b] From ^{1}H NMR analysis.[66] [c] In kg/mol, referenced to PS standards in THF. [d] M_n/M_w. [e] Recorded at 10% total mass loss under nitrogen gas, 20 °C/min. [f] Calculated from theoretical repeat unit per 1000 backbone carbons (^{1}H NMR analysis also included).

By creating polymers with pure microstructures and exact branch placement, we have synthesized a class of EP materials with unique structure and morphology.

For highly branched copolymers, the diene monomers for metathesis polymerization were synthesized as "dimers", in an ADMET sense, containing two methyl branch points per monomer. This is the first report of this synthetic methodology that lends itself well to the future creation of a variety of highly functionalized ADMET polymers. Figure 2 illustrates the monomer synthesis for diene **6**, with an abbreviated route for diene **13**. A tetraester substituted α,ω-diene **2** is produced by the dialkylation of a dibromide with the alkenyl malonate **1** forming a tetraester diene. Subsequent saponification and decarboxylation yields the diacid diene **4** which is easily converted to the diol **6** through LAH reduction. Dimesylation followed by reductive cleavage with LAH yields diene monomer **6**. Monomer **13** is produced in a similar fashion starting from alkenyl malonate and dibromobutane.

Schrock's molybdenum catalyst was chosen for the ADMET polymerization (Figure 3) due to mild metathesis conditions and recent reports concerning competitive metathesis/isomerization problems using ruthenium catalysts.[42−44]

Upon extensive purification of monomers, the polymerization was carried out in the bulk under high vacuum ($\sim 10^{-4}$ Torr). High molecular weight unsaturated copolymers, **EP5u** and **EP7u**, were isolated, and exhaustive hydrogenation yielded **EP5** and **EP7** copolymers as colorless, viscous liquids.

Molecular Weight and Structural Analysis. Polymer molecular weight and distribution were verified by GPC and NMR of both the saturated and unsaturated materials. In addition, vinyl polymer end groups and 1,2-disubstituted olefin signals visible in ^{1}H and ^{13}C NMR of the unsaturated polymers vanish upon saturation, indicating successful synthesis of saturated EP copolymers. As shown in Table 1, retention of both molecular weight and polydispersity upon hydrogenation suggests no polymer degradation during hydrogenation, and FT-IR analysis also confirms metathesis polymerization and copolymer saturation, yielding the final sequenced EP copolymers. The atactic nature of the product copolymers arises from the lack of stereocontrol during the initial polymerization of terminal olefins and a further randomization through transmetathesis reactions occurring on 1,2-disubstituted olefins along the polymer backbone. Detailed discussion concerning structural and thermal characterization for copolymers **EP5** and **EP7** follows.

Structural Analysis: ^{13}C NMR. Primary microstructural analysis for these polymers has been greatly enhanced with the application of ^{1}H and ^{13}C NMR techniques. Specifically, the ability of ^{13}C NMR to differentiate similar C−C and C−H bonding arrangements in hydrocarbon structures, such as polyolefins and paraffins, produces more structural information

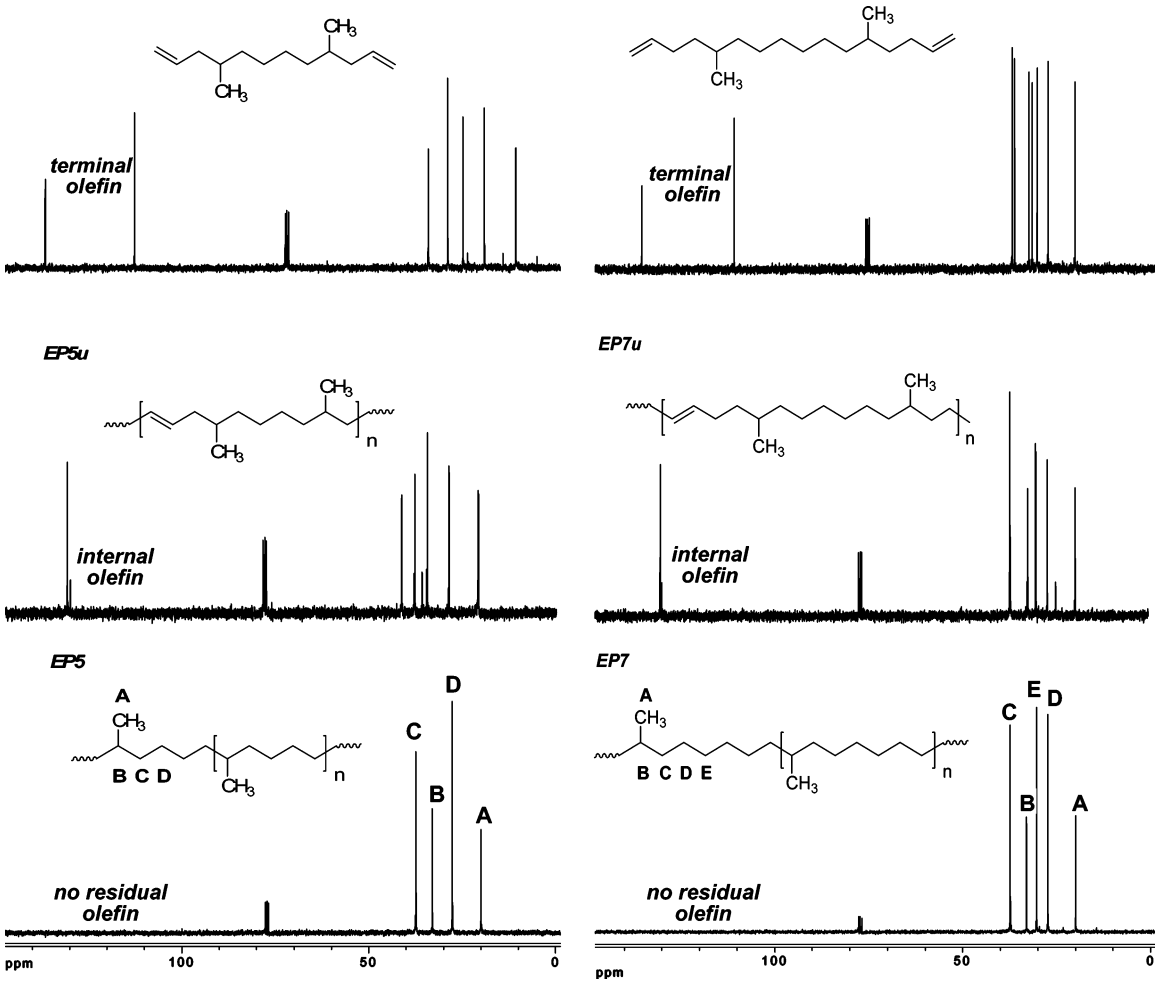

Figure 4. ^{13}C NMR analysis following monomer to copolymer for both **EP5** and **EP7**.

than ^{1}H NMR where similar chemical shifts and overlapping resonances hinder structure determination.[45] Numerous ^{13}C NMR studies of small molecule alkanes have led to a large collection of spectral data concerning individual branching arrangements for linear molecules and highly branched compounds.[45−47] Analogous polymer analysis has been performed to determine branch content,[29,48,49] branch identity,[48] and branch distribution[49,50] in a variety polyolefins.

Spectral data for **EP5** and **EP7** illustrate the structural regularity established in the precisely branched copolymers. Figure 4 depicts a side-by-side comparison of the transformations from monomer to unsaturated prepolymer to saturated EP copolymer for both **EP5** and **EP7** by ^{13}C NMR performed in $CDCl_3$. Starting in the upper left with the terminal diene containing monomer for **EP5**, signals at 115.6 and 138.0 ppm vanish when converted to high polymer, while two new signals appear corresponding to the 1,2-disubstituted double bonds along the polymer backbone as a mixture of trans (130.3 ppm, major) and cis (129.5 ppm, minor) olefins. In previous studies, the cis/trans content of typical ADMET materials was found to be ~90% trans olefin by long-scan semiquantitative ^{13}C NMR, a result attributed to the conformation of the most metallocyclobutane intermediate formed during the catalytic cycle of the metathesis polymerization.[31]

Saturation of the ADMET product greatly simplifies the ^{13}C NMR spectra, and as the signals from all olefinic and allylic carbons are removed, the precise microstructure of ADMET EP copolymers becomes apparent. For **EP5**, which contains a methyl branch on every fifth carbon, the NMR shows resonances from only four magnetically different carbons in a molecule of over 40 kg/mol arising from an axis of symmetry between the β and γ carbons from any branch point in the copolymer. Since backbone carbons C and D are twice as abundant as the methyl branch (A) and branch point carbons (B), it follows that signal intensity for carbons C and D resemble roughly twice that of carbons A and B. Upon comparison of this spectral data with previously mentioned NMR studies, our sequenced EP copolymers show good agreement with similar small molecules, but slight differences of between 0.5 and 2 ppm are seen due to the nonrepeating structure of the latter.[45] Comparison of these copolymers to methyl branched polyolefins shows excellent agreement with the branch and branch point to <1 ppm.[48,51] We postulate these small differences in chemical shift are related to the precise sequence length in our copolymers where the chemical shift of the α and β carbons are slightly altered by branches on both sides of the carbon atom in question.

Analysis of **EP7** (Figure 4) follows the same approach as terminal olefins signals are replaced with those of internal olefins. Once again, the spectrum is greatly simplified after hydrogenation, resulting in only five magnetically inequivalent carbons. In this case, the axis of symmetry resides in between the γ and δ carbon from any branch point marked as D and E, respectively. As observed with **EP5**, the branch point (B) and methyl group (A) are the least populous carbons in the material, resulting in roughly half the signal intensity relative to the other three backbone carbons (C, D, and E). Again, good agreement with small molecule studies is observed with larger discrepancies for carbon atoms further from the branch point, arising from

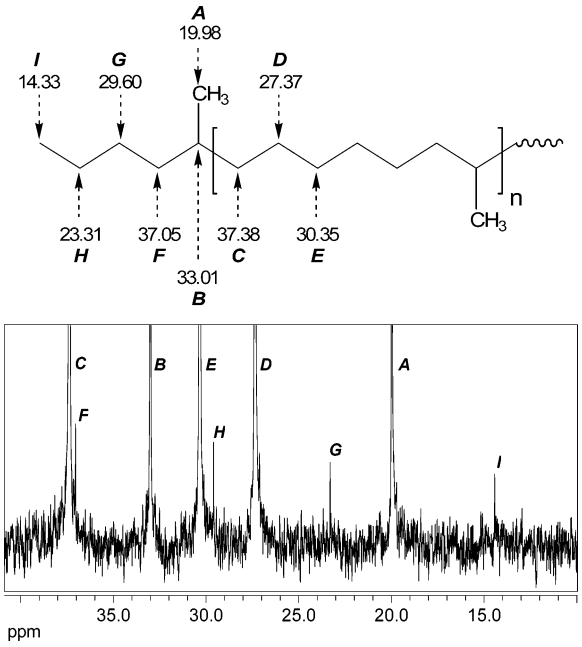

Figure 5. ^{13}C NMR end-group analysis of **EP7**.

the polymeric nature of these samples.[45] Comparison to similar methyl branched polyethylenes reveals superb agreement to reported chemical shifts to within 1 ppm.[48,51]

End-group analysis of these copolymers is also possible by ^{13}C NMR spectroscopy. Previous examination of end groups produced during ADMET polymerization have shown terminal olefins remain at chain ends[31] and, upon hydrogenation, are saturated, leaving a unique primary methyl branch[52] unlike the secondary methyl branches along the copolymer backbone of **EP5** and **EP7**. ^{13}C NMR spectroscopy of **EP7** reveals low-intensity resonances corresponding to the polymer end groups and the neighboring carbons atoms shown as an expanded view (∼100×) for the alkyl region of the spectrum (Figure 5). The large signals extending off the top of the spectrum correspond to the backbone carbon atoms with the highest molar concentration in the copolymer, while the four smaller signals labeled G, H, F, and I represent end groups and adjacent carbon atoms as labeled. These signals are easily distinguishable, and assignment as end groups agrees with our analysis of random ADMET EP materials[52] and small molecule studies mentioned earlier.[45] End-group analysis illustrates the power of ^{13}C NMR in polyolefin structure determination and supports the proposed copolymer structure for both **EP5** and **EP7**.

Structural Analysis: ^{1}H NMR. Proton NMR analysis also illustrates the microstructural control offered by the metathesis/hydrogenation methodology. Figure 6 presents a set of proton spectra tracking the conversion of diene monomer **6** to unsaturated copolymer **EP7u** to saturated copolymer **EP7**, similar to the ^{13}C NMR data presented earlier. The spectral data show the progression from the monosubstituted, terminal olefin of the monomer to the 1,2-disubstituted olefin to the saturated copolymer. The presence of cis and trans olefins in the copolymer are confirmed by the large signal at 5.39 ppm (trans) with a small shouldering signal just upfield with a maximum at 5.34 ppm (cis). As observed with ^{13}C NMR, analysis of the ^{1}H NMR spectrum for **EP7** is straightforward as only three different bonding arrangements for hydrogen exist in the copolymer: a methine, a methylene, and a methyl group. Since ^{1}H NMR can resolve the methyl group signals from the overlapping methine and methylene signals, copolymer branch content and comonomer ratios can be calculated (Table 1), but

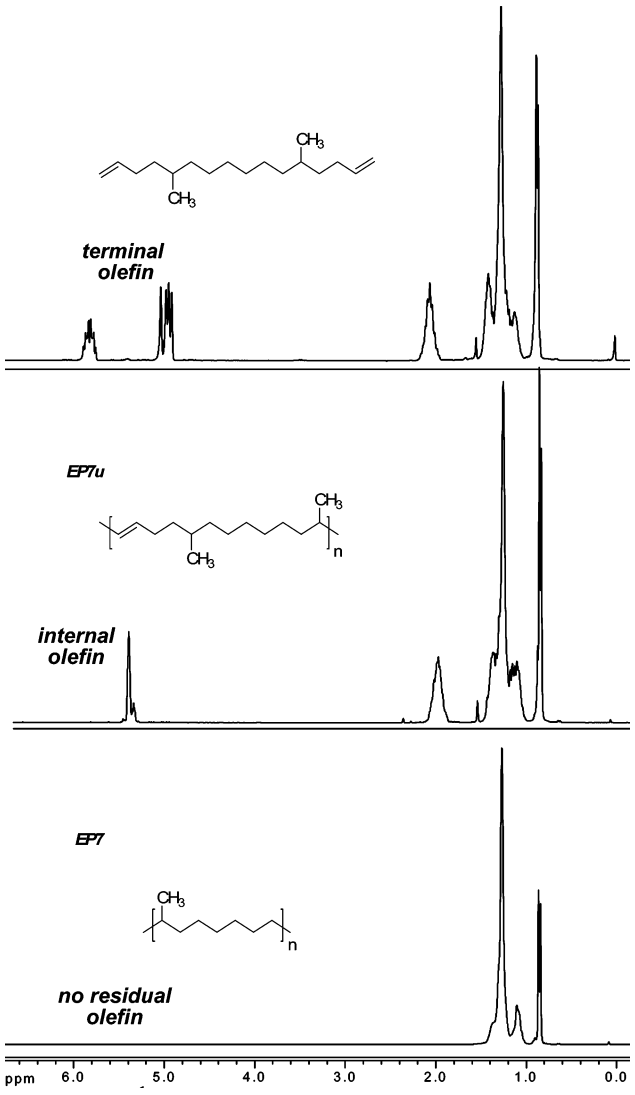

Figure 6. ^{1}H NMR analysis following monomer **6** to **EP7** sequenced ethylene−propylene copolymer.

specific bonding arrangements are difficult to deduce. As with ^{13}C NMR, ^{1}H NMR analysis for **EP5** and **EP7** supports the structural claims and proposed repeat units for both sequenced EP copolymers.

Structural Analysis: FT-IR. Structural analysis of the EP copolymers using FT-IR is a relatively straightforward analytical technique that can reveal various structural and morphological features of these materials, including crystal structure and branching content.[53,54] Previous FT-IR studies on linear paraffins and various grades of commercial PE have determined the small effects crystallization and chain-packing have on absorbance wavenumber and intensity. In most cases, especially in purely hydrocarbon systems, what may appear to be single absorbances arise from composite interactions of various methyl, methylene, and methine moieties dispersed throughout the crystalline and amorphous regions in the material.[53] While peak maxima and wavenumber may be correlated to crystal structure, or lack thereof, our **EP5** and **EP7** copolymers display absorbances from disordered morphologies associated with amorphous polymers (Figure 7).

FT-IR analysis of both unsaturated and saturated EP copolymers verifies polymerization to high molecular weight and exhaustive hydrogenation of ADMET products yielding copolymers **EP5** and **EP7**. Observable in both spectra are multiple absorbance bands between 3000 and 2800 cm^{-1} arising from

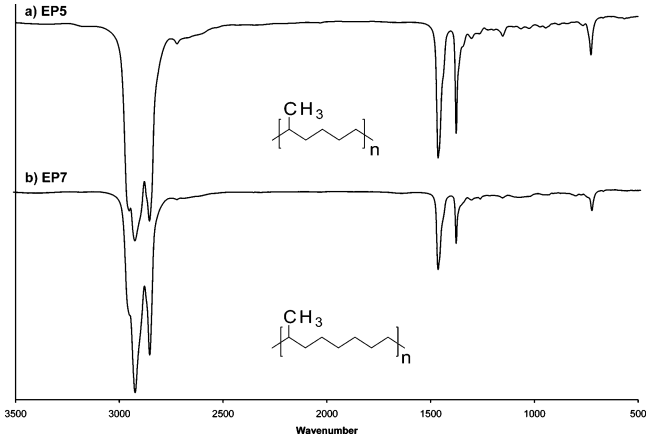

Figure 7. FT-IR analysis for sequenced EP copolymers: (a) **EP5** and (b) **EP7**.

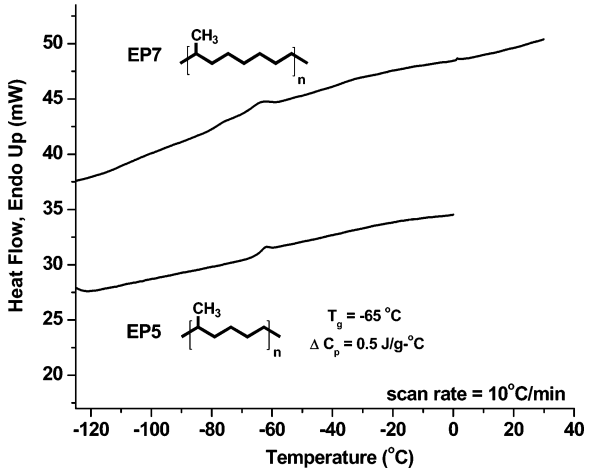

Figure 8. DSC analysis: seconding heating scan of **EP5** and **EP7**.

the abundance of methyl and methylene units in the polymer backbone. Strong bands at 2925 and 2855 cm^{-1} correspond to the methylene stretching motions from backbone carbons. For **EP5**, the shouldering peak at 2952 cm^{-1}, associated with a methyl stretch, exhibits a higher intensity than that of **EP7** due to the higher concentration of methyl branches in **EP5**. For the bands at 1464 and 1377 cm^{-1}, both copolymers show the exact same absorbance maxima corresponding to methylene and methyl bending located within a highly disordered environment,[53] and the higher methyl content in **EP5** is reflected as a greater intensity for the spectral bands at 1464 and 1377 cm^{-1} relative to methylene absorbances between 2850 and 2950 cm^{-1}. The low wavenumber band centered near 725 cm^{-1} for both copolymers corresponds to methylene rocking specifically located within an amorphous phase.[53]

Thermal Analysis: DSC. EP5 and **EP7** represent the first ever fully amorphous, sequenced copolymers produced in this fashion. Extensive thermal analysis has been performed on various academic and commercial PE materials, thereby creating a large volume of data on the subject that spans many decades. Very few reviews regarding this topic have been published in the literature,[3,55,56] and summarizing the extensive thermal data can be difficult due to both the shear number of articles and the assortment of conclusions provided therein. Herein, we have cited articles with thermal analysis of random EP copolymers of similar comonomer contents as **EP5** and **EP7** focusing on structural variations throughout various chain addition methods.

The relationship between branch content and thermal response of polymers is well documented in the literature, and thermal analysis data for various polyolefins is widely avaiable.[1,4,57] As a general rule, as short alkyl branching increases, peak melting temperatures and heats of fusion decrease until branching defects render ethylene−α-olefin copolymers amorphous, usually above 60 mol % α-olefin content.[12,56,58] For randomly copolymerized EP materials, composition charts have been developed compiling glass transition and peak melting temperatures for semicrystalline and amorphous EP copolymers based solely on comonomer ratios,[9,26] and predictions of minimum methylene sequences needed for crystallization have been reported as $n = 8$,[59] 10,[60] and 14.[21] Below this critical chain length for polymer crystallization, short methylene sequences have been linked to a low-temperature relaxation where $T < T_g$: $n = 2$,[61] 3,[62] and ≥ 2[56] for $T_\gamma = -125$ °C. While the true glass transition temperature of PE has been debated due to multiple detectable polymer relaxations,[56] random EP materials exhibit composite thermal responses from PE-like and polypropylene-like polymer segments throughout the material,[9,18,21] making it difficult to discern which structural features are causing specific thermal events. The synthetic methodology applied creates macromolecular architectures with defined repeat units generating perfectly sequenced EP materials that offer the ability to directly probe the effects of specific branch (defect) placement on polymer morphology and crystal structure.

Differential scanning calorimetry (DSC) was performed on a series of sequenced ADMET EP copolymers to determine the effects of exact ethylene run lengths on thermal response. All previously synthesized examples of ADMET EP copolymers (EP9, -11, -15, -19, and -21)[7,8,35] exhibit semicrystalline behavior with a common trend of increasing peak melt temperature and heat of fusion with increasing ethylene run length or decreasing branch content (Figure 1). Although these data are in good agreement with thermal data from the corresponding randomly branched EP materials, ADMET EP copolymers display sharp, well-defined melting endotherms unlike statistical EP copolymers, which usually exhibit long, broad melting endotherms due to a the latter having a distribution of ethylene sequence lengths and polydisperse lamellae thicknesses.[21] Sequenced EP copolymers having exact ethylene run lengths lead to a regular repeating polymer structure, allowing more uniform crystallite formation and lamellar thickness distribution. The β glass transition temperatures for all semicrystalline ADMET EP sequenced copolymers have been recorded at −43 °C for ethylene run lengths of $n = 8-20$ regardless of branch density.[35]

DSC experiments on **EP5** and **EP7** were performed at a scan rate of 10 °C/min from −120 to 150 °C, and the second heating curves for the two new additions to this family of EP materials are displayed in Figure 8. For **EP5**, a single, clearly defined relaxation can be observed at −65 °C with a ΔC_p of 0.5 J/(g °C). This transition has been assigned as the glass transition temperature for this copolymer and is roughly 22 °C lower than previous examples of sequenced EP copolymers.[35] In comparison with literature data for random EP copolymers, a number of examples exhibit thermal relaxations near this temperature and have been assigned as glass transitions.[12,17−19,21,26,63] The shift of this relaxation of **EP5** to a lower temperature relative to previous perfectly sequenced EP copolymers[35,40,64] is attributed to a higher methyl branch density inhibiting polymer chain flexibility as seen in examples random EP materials also;[26] **EP5** represents the first example of a completely amorphous, sequenced EP copolymer within this family of precisely branched materials. We have isolated the branch content necessary to block crystallization in a sequenced EP material or, in other words, determined the smallest crystallizable ethylene run length at six carbons.

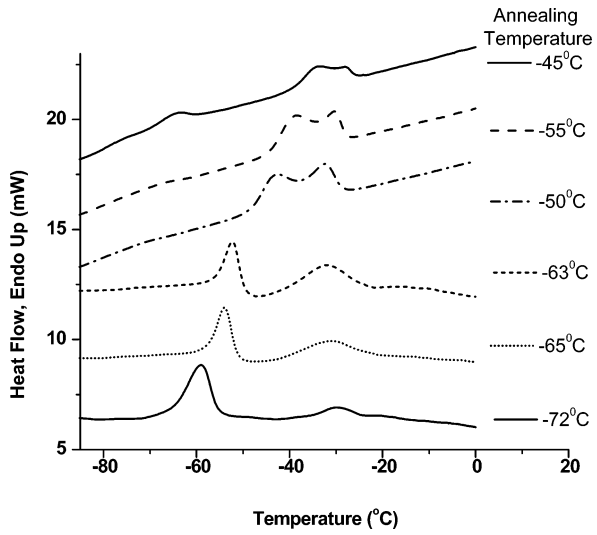

Figure 9. DSC curves for annealing experiments on **EP7**.

For **EP7**, the second heating curve of the experiment at 10 °C/min illustrates the long, broad endothermic response occurring over a large temperature range of 120 °C (Figure 8). This observation was attributed to an initial polymer relaxation at −110 °C followed by a secondary relaxation at −80 °C overlapping with a possible broad melting event. Concurrent and/or consecutive relaxations and polymer melts are common in highly branched EP materials and are illustrated well by Ferrari,[12] Reynaers,[17] and Sozzani.[20] One notable difference in the thermal response of our sequenced **EP7** copolymer is the initial relaxation at −110 °C being close to the reported T_γ transition at −125 ± 10 °C.[56] While this relaxation has been attributed to long, pendant alkyl branch motion, we observe similar low-temperature relaxations in a copolymer with a methylene sequence of six carbons and only methyl branches. Unlike previous examples of randomly copolymerized EP materials of roughly 70 mol % ethylene,[17,21,26] the initial relaxation for **EP7** at −110 °C occurred roughly 20 degrees lower than the reported range of −60 to −40 °C. Since previous examples of methyl branched ADMET EP copolymers only displayed transitions at −43 °C, corresponding to the β-glass transition; this lead us to believe we could discount the methyl branches for this low-temperature relaxation, but specific literature data suggest this −110 °C transition arises from methyl branch rotation.[65] Considering the relaxation data from **EP5** exhibits no such transition, we can relate the methylene sequence of $n = 6$, corresponding to three sequential ethylene units, to the −110 and −80 °C relaxations, and a few examples from statistical EP systems support this conclusion.[18]

To further resolve the thermal response of **EP7**, various 1 h annealing treatments between −72 and −40 °C were performed to isolate specific transitions. Using a DSC, the material was held isothermally for 1 h, quench cooled to −120 °C, and heated from −120 to 50 °C at a scan rate of 10 °C/min. The thermal responses of **EP7** upon thermal treatments at various temperatures are given in Figure 9. After annealing **EP7** at −72 °C, two endotherms appear at −60 °C (major) and −30 °C (minor) with peak shapes suggesting the melting of polymeric crystals rather than chain relaxations, but notably, two different polymorphs due to multiple transitions. Annealing at −65 °C shifts the lower temperature peak to −54 °C while the second peak is slightly expanded and broadened. The trend continues when annealed at −63 °C as the first peak recedes slightly and the second increases in peak area. Also, a noted exotherm between the two endothermic transitions suggests a melting−recrystallization event, dynamically reordering the polymer chains into a higher melting crystal form during the experiment. At higher temperatures of −50 and −55 °C, the two endotherms merge into a bimodal response centered near −40 °C. Annealing at −45 °C shows the reappearance of both lower temperature endotherms near −80 and −60 °C, although the bimodal melt still prevails as the strongest transition at −30 °C. In the final experiment, **EP7** was held annealed at −40 °C, but the sample exhibited an identical thermal response to that of the initial DSC experiment (Figure 8) under dynamic scanning conditions and no previous annealing performed. The bimodal melting after assorted thermal annealing treatments, along with broad thermal response under dynamic scanning, supports the hypothesis that the high methyl branch density in **EP7** forces the material into a metastable state where chain packing is encumbered, thus generating conformationally disordered and highly strained crystalline domains.

Crystal structure analysis of EP21 and EP15 using X-ray powder diffraction data was recently reported, indicating a mixed hexagonal−triclinic crystal arrangement in EP15 and EP21 copolymers.[7] Because of the regularity of the copolymer structures and the ability of longer ethylene run lengths to crystallize, secondary structure characterization suggests that the chain stems nucleate to form staggered, triclinic arrangements that are able to include methyl branches within the lamellae, while simultaneously providing a mechanism for backbone methylenes to order via a hexagonal sublattice.

Drawing from these results, we believe similar events are taking place during low-temperature **EP7** crystallization. However, owing to the higher degree of branch content of **EP7,** several ill-defined thermal transitions were encountered that indicate that the various crystal forms are both less dense and less stable when compared to the EP15 and EP21 materials described by Lieser et al.[7] According to our earlier analysis, as ethylene sequence length is decreased, conformational disorder in ADMET EP copolymers is increased, leading to lower density copolymers with less hexagonal character and more defective triclinic arrangements. Revisiting previously discussed thermal analysis (Figure 1), the response of **EP7** seems intuitive as **EP5** is completely amorphous, and **EP9** is a very low-density semicrystalline polymer. The intermediate branch density in **EP7** impedes crystallite formation unless specific thermal treatments are applied, thus supporting formation of various thermodynamically metastable states that cannot be observed under dynamic scanning.

For a copolymer containing a run length of shorter than four methylene groups between methyl branches, the only observed transition for **EP5** is a clearly defined T_g at −65 °C and a ΔC_p of 0.5 J/g, with no melting event detected—even upon annealing at various low temperatures. If **EP5** has too many branches to crystallize and **EP9** has the lowest peak melting temperature of the family, the behavior of **EP7** can be explained by branch content alone. At this propylene content, sequenced materials contain an even distribution of methyl defects throughout the copolymer backbone, thereby requiring a methylene sequence of seven or more for crystallization to occur. The development of multiple endotherms and bimodal melting for **EP7** can likely be attributed to various low-density crystals with packing arrangements similar to previously analyzed ADMET materials. Hence, **EP7** seems to fall on the boundary of crystalline and amorphous polymers in our family of sequenced EP copolymers; this indicates that the smallest crystallizable run length between branches is between $n = 5$ and 8 methylene units, similar to previous predictions and reports described earlier.

Conclusion

In summary, by applying a new synthetic approach to diene monomer synthesis, two sequenced EP copolymers have been synthesized through a sequential ADMET polymerization/hydrogenation methodology. ADMET EP copolymers were analyzed by FT-IR, ^{1}H NMR, and GPC. ^{13}C NMR was used for to perform in-depth structural investigation and end-group analysis in order to assign exact chemical shifts for specific methyl branching patterns and sequence lengths in EP copolymers. Methyl branch contents and distributions were controlled through metathesis polymerization, and targeted copolymers were attained in good yield. This approach to EP copolymer synthesis yields precise model polyolefins that are used to isolate explicit structural features in a single material without the problems associated with multiple-branch identities and variable-comonomer distributions observed in most chain addition materials.

Thermal analysis of sequenced EP copolymers revealed the first amorphous example to date, **EP5**, exhibiting a glass transition temperature of −65 °C and a $\Delta C_p = 0.5$ J/(g °C). Both **EP5**, with four carbons between branch points, and **EP7**, with six carbons between branch points, exhibit amorphous character under dynamic scanning calorimetry at 10 °C/min; however, annealing experiments carried out at low temperatures for **EP7** reveal ill-defined endothermic thermal responses that indicate the presence of, disordered, metastable crystalline regimes in this material. Future applications of this synthetic methodology include the investigation of longer alkyl branches and longer ethylene sequence lengths in similar polyolefin copolymers.

Acknowledgment. The authors thank the Florida Space Grant Consortium (NASA-FSGC) and the National Science Foundation (NSF) for financial support as well as the Army Research Office (ARO) for its support of catalyst development.

References and Notes

(1) Alamo, R. G.; Mandelkern, L. *Macromolecules* **1989**, *22*, 1273−1277.
(2) Bubeck, R. A. *Mater. Sci. Eng., R* **2002**, *39*, 1−28.
(3) Ungar, G.; Zeng, X. B. *Chem. Rev.* **2001**, *101*, 4157−4188.
(4) Alamo, R. G.; Mandelkern, L.; Stack, G. M.; Kronke, C.; Wegner, G. *Macromolecules* **1994**, *27*, 147−156.
(5) Ruiz de Ballesteros, O.; Auriemma, F.; Guerra, G.; Corradini, P. *Macromolecules* **1996**, *29*, 7141−7148.
(6) VanderHart, D. L.; Pereze, E. *Macromolecules* **1986**, *19*, 1902−1909.
(7) Lieser, G.; Wegner, G.; Smith, J. A.; Wagener, K. B. *Colloid Polym. Sci.* **2004**, *282*, 773−781.
(8) Qiu, W.; Sworen, J.; Pyda, M.; Nowak-Pyda, E.; Habenschuss, A.; Wagener, K. B.; Wunderlich, B. *Macromolecules* **2006**, *39*, 204−217.
(9) Burfiled, D. R. *Macromolecules* **1985**, *18*, 2684−2688.
(10) Alizadeh, A.; Richardson, L.; Xu, J.; McCartney, S.; Marand, H.; Cheung, Y. W.; Chum, S. *Macromolecules* **1999**, *32*, 6221−6235.
(11) Zhang, F.; Song, M.; Lu, T.; Liu, J.; He, T. *Polymer* **2002**, *43*, 1453−1460.
(12) Pizzoli, M.; Righetti, M. C.; Vitali, M.; Ferrari, P. *Polymer* **1998**, *39*, 1445−1451.
(13) Odian, G. *Principles of Polymerization*, 4th ed.; John Wiley & Sons: New York, 2004.
(14) Sueo Machi, S. K. M. H. T. K. *J. Polym. Sci., Part A-1: Polym. Chem.* **1967**, *5*, 3115−3128.
(15) Philipp Becker, M. B. J. S. *Macromol. Chem. Phys.* **2002**, *203*, 2113−2123.
(16) Gassman, P. G.; Callstrom, M. R. *J. Am. Chem. Soc.* **1987**, *109*, 7875−7876.
(17) Eynde, S. V.; Mathot, V.; Koch, M. H. J.; Reynaers, H. *Polymer* **2000**, *41*, 3437−3453.
(18) Starkweather, J. H. W. *Macromolecules* **1980**, *13*, 892−897.
(19) Wright, K. J.; Lesser, A. J. *Macromolecules* **2001**, *34*, 3626−3633.
(20) Bracco, S.; Comotti, A.; Simonutti, R.; Camurati, I.; Sozzani, P. *Macromolecules* **2002**, *35*, 1677−1684.
(21) Burfield, D. R.; Kashiwa, N. *Makromol. Chem.* **1985**, *186*, 2657−2662.
(22) Alt, H. G.; Koppl, A. *Chem. Rev.* **2000**, *100*, 1205−1222.
(23) Tynys, A.; Saarinen, T.; Hakala, K.; Helaja, T.; Vanne, T.; Lehmus, P.; Löfgren, B. *Macromol. Chem. Phys.* **2005**, *206*, 1043−1056.
(24) DeRosa, C.; Auriemma, F. *Macromolecules* **2006**, *39*, 249−256.
(25) Piel, C.; Karssenberg, F. G.; Kaminsky, W.; Mathot, V. B. F. *Macromolecules* **2005**, *38*, 6789−6795.
(26) Mader, D.; Heinemann, J.; Walter, P.; Mulhaupt, R. *Macromolecules* **2000**, *33*, 1254−1261.
(27) Ittel, S. D.; Johnson, L. K.; Brookhart, M. *Chem. Rev.* **2000**, *100*, 1169−1204.
(28) Gates, D. P.; Svejda, S. A.; Onate, E.; Killian, C. M.; Johnson, L. K.; White, P. S.; Brookhart, M. *Macromolecules* **2000**, *33*, 2320−2334.
(29) Johnson, L. K.; Killian, C. M.; Brookhart, M. *J. Am. Chem. Soc.* **1995**, *117*, 6414−6415.
(30) Baughman, T. W.; Wagener, K. B. *Rec. Adv. ADMET Polym.* **2005**, 1−42.
(31) Lehman, S. E.; Wagener Kenneth, B. ADMET Polymerization. In *Handbook of Metathesis*; Grubbs, R. H., Ed. Wiley-VCH: New York, 2003; Vol. 3, pp 283−353.
(32) Matloka, P. P.; Sworen, J. C.; Zuluaga, F.; Wagener, K. B. *Macromol. Chem. Phys.* **2005**, *206*, 218−226.
(33) Hopkins, T. E.; Wagener, K. B. *Macromolecules* **2004**, *37*, 1180−1189.
(34) Hopkins, T. E.; Wagener, K. B. *J. Mol. Catal. A: Chem.* **2004**, *213*, 93−99.
(35) Smith, J. A.; Brzezinska, K. R.; Valenti, D. J.; Wagener, K. B. *Macromolecules* **2000**, *33*, 3781−3794.
(36) Sworen, J. C.; Smith, J. A.; Berg, J. M.; Wagener, K. B. *J. Am. Chem. Soc.* **2004**, *126*, 11238−11246.
(37) Sworen, J. C. Modeling linear-low-density polyethylene: copolymers containing precise structures. University of Florida, Gainesville, 2004.
(38) Schrock, R. R.; Murdzek, J. S.; Bazan, G. C.; Robbins, J.; DiMare, M.; O'Regan, M. *J. Am. Chem. Soc.* **1990**, *112*, 3875−3886.
(39) Molander, G. A.; Harris, C. R. *J. Am. Chem. Soc.* **1996**, *118*, 4059−4071.
(40) Wagener, K. B.; Valenti, D.; Hahn, S. F. *Macromolecules* **1997**, *30*, 6688−6690.
(41) Minick, J.; Moet, A.; Hiltner, A.; Baer, E.; Chum, S. P. *J. Appl. Polym. Sci.* **1995**, *58*, 1371−1384.
(42) Lehman, S. E.; Schwendeman, J. E.; O'Donnell, P. M.; Wagener, K. B. *Inorg. Chim. Acta* **2003**, *345*, 190−198.
(43) Formentin, P.; Gimeno, N.; Steinke, J. H. G.; Vilar, R. *J. Org. Chem.* **2005**, *70*, 8235−8238.
(44) Bernd, S. *Eur. J. Org. Chem.* **2003**, 816−819.
(45) Lindeman, L. P.; Adams, J. Q. *Anal. Chem.* **1971**, *43*, 1245−1252.
(46) Goldstein, J. H.; Tarpley, J. A. R.; Carman, C. J. *Macromolecules* **1973**, *6*, 719−724.
(47) Grant, D. M.; Paul, E. G. *J. Am. Chem. Soc.* **1964**, *86*, 2984−2990.
(48) Axelson, D. E.; Levy, G. C.; Mandelkern, L. *Macromolecules* **1979**, *12*, 41−52.
(49) Jurkiewicz, A.; Eilerts, N. W.; Hsieh, E. T. *Macromolecules* **1999**, *32*, 5471−5476.
(50) Hsieh, E. T.; Randall, J. C. *Macromolecules* **1982**, *15*, 353−360.
(51) Randall, J. C. *J. Polym. Sci., Polym. Phys. Ed.* **1973**, *11*, 275−287.
(52) Sworen, J. C.; Smith, J. A.; Wagener, K. B.; Baugh, L. S.; Rucker, S. P. *J. Am. Chem. Soc.* **2003**, *125*, 2228−2240.
(53) Krimm, S.; Liang, C. Y.; Sutherland, G. B. B. M. *J. Chem. Phys.* **1956**, *25*, 549−562.
(54) Tashiro, K.; Sasaki, S.; Kobayashi, M. *Macromolecules* **1996**, *29*, 7460−7469.
(55) Gedde, U. W.; Mattozzi, A. *Polyethylene Morphology* **2004**, 29−74.
(56) Boyer, R. F. *Macromolecules* **1973**, *6*, 288−299.
(57) Flory, P. J. *Trans. Faraday Soc.* **1955**, *51*, 848−857.
(58) Maurer, J. J. *Rubber Chem. Technol.* **1965**, *38*, 979−990.
(59) Richardson, M. J.; Flory, P. J.; Jackson, J. B. *Polymer* **1963**, *4*, 221−236.
(60) Baldwin, F. P.; ver Strate, G. *Rubber Chem. Technol.* **1972**, *45*, 709−881.
(61) Boyer, R. F. *Rubber Chem. Technol.* **1963**, *36*, 1303−1421.
(62) Wunderlich, B. *J. Chem. Phys.* **1962**, *37*, 2429−2432.
(63) Burfiled, D. R.; Kashiwa, N. *Makromol. Chem.* **1985**, *186*, 2657−2662.
(64) Sworen, J. C.; Smith, J. A.; Wagener, K. B.; Baugh, L. S.; Rucker, S. P. *J. Am. Chem. Soc.* **2003**, *125*, 2228−2240.
(65) McCall, D. W. *Acc. Chem. Res.* **1971**, *4*, 223−232.
(66) Equation for NMR comonomer ratio determination: mol % propylene = #propylene/(#propylene + #ethylene) = $(A/3)/[A/3 + (B - A)/4]$, where A = integral value of 0.9 ppm signal (propylene methyl group) and B = integral value of broad 1.0−1.4 ppm signal (all other protons).

MA0602876